CNS Neuroscience & Therapeutics

ORIGINAL ARTICLE

CNS Neuroscience & Therapeutics

Psora-4, a Kv1.3 Blocker, Enhances Differentiation and Maturation in Neural Progenitor Cells

Yu-Ye Zhou,[1] Guo-Qiang Hou,[1] Song-Wei He,[1] Zhuo Xiao,[1] Hui-Juan Xu,[1] Ya-Tao Qiu,[2] Sheng Jiang,[2] Hui Zheng[1] & Zhi-Yuan Li[1,3]

1 Key Laboratory of Regenerative Biology, South China Institute of Stem Cell and Regenerative Medicine, Guangzhou Institutes of Biomedicine and Health, Chinese Academy of Sciences, Guangzhou, Guangdong, China
2 Institute of Chemical Biology, Guangzhou Institutes of Biomedicine and Health, Chinese Academy of Sciences, Guangzhou, Guangdong, China
3 Department of Anatomy and Neurobiology, School of Basic Medical Sciences, Central South University, Changsha, Hunan, China

Keywords
Differentiation; Kv1.3; Maturation; Neural progenitor cell; Small molecule.

Correspondence
Z-Y. Li, Guangzhou Institutes of Biomedicine and Health, #190 Kaiyuan Avenue, Science Park, Guangzhou 510530, Guangdong, China.
Tel.: +86-20-3201-5241;
Fax: +86-20-3201-5299;
E-mail: li_zhiyuan@gibh.ac.cn
Received 7 January 2015; revision 12 April 2015; accepted 14 April 2015

doi: 10.1111/cns.12402

SUMMARY

Aim: The self-repair ability of neural progenitor cells (NPCs) has been found to be activated and protected in several therapies helpful in multiple sclerosis (MS), an inflammatory demyelinating disease of the CNS. As a potential therapeutic target in MS, the role of the ion channel Kv1.3 in NPC self-repair has received limited attention. The aim of this study was to explore the effects of a selective Kv1.3 blocker on NPC neuronal differentiation and maturation. **Methods:** A small-molecule selective blocker for Kv1.3, Psora-4, was added to the differentiation medium of cultured mouse NPCs to assess its effect on NPC differentiation efficiency. Both a polypeptide Kv1.3 blocker and Kv1.3-specific RNA interference were used in parallel experiments. Further, the maturity of newborn neurons in the presence of Psora-4 was measured both by morphological analysis and by whole-cell patch clamping. **Results:** Psora-4 induced a significant increase in the percentage of neurons. Knockdown of Kv1.3 in NPCs also promoted neuronal differentiation. Both morphological and electrophysiological analyses suggested that NPC-derived neurons in the presence of Psora-4 were more mature. **Conclusion:** Our studies reveal a crucial role for the ion channel Kv1.3 in the regulation of NPC differentiation and maturation, making Psora-4 a promising candidate molecule for MS treatment.

Introduction

Neural progenitor cells (NPCs), also known as neural stem cells, exist in both the developing and the adult central nervous system (CNS) in all mammals [1]. Because of their capacity to self-renew, proliferate, and differentiate, NPCs have been explored for their potential in treating CNS disorders such as multiple sclerosis (MS). MS is an inflammatory demyelinating disease that results in cumulative and irreversible CNS damage and for which there is no known cure [2–5]. Recently, studies in animal models of MS showed that NPCs were activated as part of CNS self-repair [6]. Transplantation of neural stem cells or nestin-positive neural precursor cells from adult brain resulted in functional remyelination, which indicates the potential therapeutic value of NPCs for MS [7,8]. Moreover, the self-repair capacity of NPCs was found to be activated and protected in some MS therapies, such as drug therapy targeting Kv1.3 and therapy based on mesenchymal stem cell engraftment [9–11]. These studies suggest a potential role for NPCs in MS treatment. However, the mechanism still needs more supporting evidence.

Kv1.3 is a Shaker-type, delayed-rectifier potassium channel [12], and it is functionally active in lymphocytes, cancer cells, and neurocytes [13–16]. Kv1.3-selective blockers had been reported to be an effective treatment for MS [17]. However, most of these studies focused on the immunosuppressive effect of Kv1.3 blockers and neglected the effects on NPCs. Recently, Kv1.3 blockers were reported to attenuate the neurotoxicity caused by activated T cells in neuro-inflammatory diseases [18,19]. In addition, Kv1.3 ($^{-/-}$) mice showed changed proportions of interneuron subtypes [20]. These findings revealed a potential role for Kv1.3 in neuronal differentiation.

Psora-4, a 5-phenylalkoxypsoralen, is the most potent small-molecule Kv1.3 inhibitor which with relatively simple structure and low molecule weight in comparison with traditional polypeptide blocker such as margatoxin (MgTX) [21]. Its selectivity for Kv1.3 is 17- to 70-fold higher than most related Kv1-family channels (e.g., Kv1.1, Kv1.2, Kv1.4, and Kv1.7). Psora-4 blocked Kv1.3 in a dose-dependent manner by binding to the C-type inactivated state of the channel, with an EC_{50} value of 3 nM [22].

In the present study, we found that Kv1.3 selective blockers, either Psora-4 or MgTX, increased the proportion of β-III-tubulin-positive neurons among mouse NPC differentiation progenies. Selective silencing of Kv1.3 in NPCs through RNA interference also promoted neuronal differentiation. Furthermore, we found

that neurons differentiated in the presence of Kv1.3 blockers developed a more mature morphology. Patch-clamp recordings suggested that Psora-4 induced newborn neurons to develop more mature electrophysiological functions. Our results indicate that Kv1.3 blockade or silencing could promote NPC neuronal differentiation and maturation. Psora-4, as a non-toxic small molecule, could be developed into a promising clinical therapeutic drug for MS treatment.

Materials and Methods

Cell Culture

Animals were handled according to protocols that were approved by the Guangzhou Institutes of Biomedicine and Health Committee on Animal Care and that are in accordance with national guidelines. Primary NPCs were prepared from fetal mice at embryonic Day 13. Briefly, a pregnant mouse was decapitated under chloroform anesthesia, and the embryos were removed from the uterus. Then, their brains were isolated, and the cerebral cortex was collected using surgical scissors. The collected tissue was then gently triturated, washed in PBS (1×), and digested in trypsin (0.05%; Life Technologies, Gaithersburg, MD, USA) for 15 min at 37°C. The digested tissue was subsequently centrifuged, washed twice with PBS, and homogenized to single-cell suspension by gentle trituration. Then, cells were plated in cell culture flasks (Nunc) and incubated at 37°C in an atmosphere of 5% CO_2 in air. The proliferation medium contained 97% Dulbecco's modified Eagle's medium/nutrient mixture F-12, 1% N2 supplement, 2% B27 supplement (all from Life Technologies) and was supplemented with 20 ng/mL epidermal growth factor (EGF), 20 ng/mL recombinant human fibroblast growth factor-basic (bFGF, both from PeproTech, Rocky Hill, NJ, USA) to maintain neurosphere proliferation [23]. After 3 days, the cells formed neurospheres. At 3-day intervals, the neurospheres were passaged by dissociation into single cells. Unless otherwise indicated, all the experiments were carried out with NPCs at passages 8–10.

For NPC differentiation, single NPCs were plated in 24-well plates coated with Matrigel (BD Biosciences, Franklin Lakes, NJ, USA) at 10×10^4 cells per well. At 24 h after plating, the medium was replaced with differentiation medium containing Psora-4 or MgTX (Sigma-Aldrich, St. Louis, MO, USA) at the indicated concentration, and the medium was refreshed each day. Differentiation medium does not contain the bFGF and EGF found in proliferation medium, but instead contains 10 ng/mL brain-derived neurotrophic factor (BDNF; PeproTech) and 1 μM cyclic adenosine monophosphate (cAMP; Sigma-Aldrich) to improve neuronal survival [23]. Unless otherwise indicated, Psora-4 was added into the differentiation medium at 10 nM.

Immunocytochemistry

Cells were fixed in 4% paraformaldehyde for 13 min. After permeabilization with 0.2% Triton X-100 in PBS (PBST) for 10 min, the cells were blocked with 10% goat serum in PBS for 30 min. Next, the cells were incubated in primary antibody solution (10% goat serum with the indicated primary antibody in PBST) for 1 h at room temperature or overnight at 4°C. The following monoclonal antibodies were used: rabbit anti-β-III-tubulin (1:500; Merck Millipore, Darmstadt, Germany), mouse anti-glial fibrillary acidic protein (GFAP, 1:1000; Merck Millipore), mouse antimicrotubule-associated protein 2 (MAP2, 1:400; Merck Millipore), and rat antinestin (1:100; Merck Millipore). After cells were washed in PBST for three times, they were incubated with secondary antibodies conjugated with anti-mouse Alexa Fluor 555 and anti-rabbit Alexa Fluor 488 (both from Cell Signaling Technology, Beverly, MA, USA) in PBS with 5% goat serum for 1 h at room temperature, followed by nuclear staining with 4′,6-diamidino-2-phenylindole (DAPI) for 5 min. Images were acquired with an inverted fluorescence microscopy system (LEICA DMI6000B, Wetzlar, Germany) or a confocal system (Single-photon Zeiss 710 NLO, Jena, Germany).

Electrophysiological Recordings

Matrigel-coated coverslips with differentiated NPC progeny at days 5–10, 13–16, and 20–24 were subjected to electrophysiological recording. The coverslip was placed in a perfusion chamber before measurement and immersed in bath solution containing (in mM): 127 NaCl, 3 KCl, 1 $MgSO_4$, 26 $NaHCO_3$, 1.25 NaH_2PO_4, 1 D-glucose (1 H_2O), 2 $CaCl_2$, pH adjusted to 7.4 with HCl. Recording pipettes were fabricated from borosilicate glass using a Flaming–Brown puller (model P-97; Sutter Instruments, Novato, CA, USA), and the final resistances were 6–10 MΩ. The pipette solution contained (in mM): 140 potassium methanesulfonate, 5 NaCl, 1 $CaCl_2$, 10 HEPES, 0.2 EGTA, 3 ATP, and 0.4 GTP, pH 7.4 with KOH. Neurons were identified based on neuronal morphology and the ability to fire action potentials. Whole-cell patch-clamp recordings were carried out with patch-clamp amplifiers (Axopatch) and pClamp 10.2 (Axon Instruments, Sunnyvale, CA, USA) as the data acquisition and analysis software.

To examine the excitability of neurons, transient membrane currents induced by stepping the holding membrane potential from −80 mV to +80 mV (500 ms) were recorded. Then, the cell was switched to current-clamp mode, and currents (−20 pA to 50 pA, 300 ms) were injected through the patch pipette to examine whether action potentials could be induced. Spontaneous action potentials were collected during a 10-min period of continuous recording in current-clamp mode (0 pA) and then analyzed.

shRNA Silencing of Kv1.3 in NPCs

The third-generation lentiviral vector pSicoR-mCherry was used to construct the shRNA expression system. Four sequences designed against Kv1.3, and one Nonsense control was inserted separately into the vector (Table 1). The empty lentiviral expression vector was also used as a Blank vector control.

For viral packaging, the shRNA-expressing lentiviral plasmid was co-transfected with plasmids pMD2G and pSPAX2 into 293T cells. Virus-containing medium was collected and filtered at 48 h and 72 h after transfection. Viral titers were measured by serial dilution on 293T cells and estimated after 72 h.

For viral transduction, NPCs were adhered to Matrigel for 2 h, followed by incubation with lentivirus-containing medium at a multiplicity of infection of 10. Medium was replaced with NPC

Table 1 Oligonucleotide sequences used for generation of shRNA vectors

shRNA	Sense	Loop	Antisense
shRNA-1	TCTGAGTAAGTCGGAGTATAT	TTCAAGAGA	ATATACTCCGACTTACTCAGA
shRNA-2	GCATTGCCAGTTCCTGTGATT		AATCACAGGAACTGGCAATGC
shRNA-3	CGACGCCATCCTCTACTACTA		TAGTAGTAGAGGATGGCGTCG
shRNA-4	AGGTGTCTTGACCATTGCATT		AATGCAATGGTCAAGACACCT
Nonsense	CAACAAGATGAAGAGCACCAA		TTGGTGCTCTTCATCTTGTTG

Four shRNA-Kv1.3 sequences and one Nonsense control sequence were applied. Each hairpin was constructed from the sense strand followed by the loop and then the antisense strand.

proliferation medium at 12 h after transduction. After 72 h, cells were digested to a suspension and then passaged.

For cell purification, shRNA-transduced neurospheres were digested into single-cell suspensions. After filtration with a 40-μm filter (BD Biosciences), cells were sorted using fluorescence-activated cell sorter (FACS Aria IIU; BD Biosciences). After several passages, the purified cells were subjected to real-time quantitative PCR to estimate the knockdown efficiency.

Real-time Quantitative PCR

Total RNA was extracted using TRIzol reagent (Invitrogen, Life Technologies, Grand Island, NY, USA). Total cDNA was prepared with PrimeScript RT Reagent Kit Perfect Real Time (Takara, Shiga, Japan) and used as templates for PCR. PCR reagents and SYBR Green Premix EX Taq™ (Takara) were used with forward and reverse primers (2.5 nM). Real-time quantitative PCR was performed with the CFX96™ Real-time PCR (Bio-Rad, Hercules, CA, USA). β-actin was used as an internal control. The Kv1.3/β-actin ratio of every sample was calculated, and the results were expressed as a percentage of the Nonsense control group in the shRNA experiments. All amplifications were performed in duplicate, and at least three technical and three biological replicates were performed. PCR primer sequences were as follows: Kv1.3, forward 5′-tactttgacccactccgcaa, reverse 5′-tggtaaaagcggatctcctcg; β-actin, forward 5′-ccttcttgggtatggaatcctgt, reverse 5′-tttacggatgt caacgtcacac.

Chemical Synthesis

First, 50 mg 4-methoxy-7H-furo[3,2-g]chromen-7-one was reacted at −20°C with boron tribromide (0.95 mL) in a solution of CH_2Cl_2 (1.5 mL) under a protective argon. The progress of the reaction was monitored by thin-layer chromatography. After the completion of the reaction, the product mixture was applied to posttreatment and concentrated to dryness. Next, this product (25 mg) was reacted with (4-bromobutyl)-benzene (0.03 mL) in the presence of the catalysts sodium iodide (7.2 mg) and potassium carbonate (49.7 mg) under reflux in the solvent dimethyl formamide (DMF, 2 mL) and under argon protection. The reaction was completed after 4 h. Then, Psora-4 was dissociated under column chromatography (23 mg, 65%). The compound was characterized by melting point and ^{1}H NMR analyses, in which the data corresponded to the reference [22].

Statistical Analysis

To calculate the efficiency of differentiation, the total number of cells and immunolabeled cells were counted from seven random fields of view per coverslip. For mature neuron candidates, all of the cells on the coverslip were counted. Both types of counting were performed under a fluorescence microscope with a 20× objective. For neuron morphology calculating, the longest neurite length and the number of branches were measured for each β-III-tubulin-positive cell. At least three independent experiments were performed. Data were graphed using OriginPro 8 software (OriginLab, Northampton, MA, USA). Mean values and the standard error were calculated for each treatment group. Statistical analysis was performed using SPSS (Statistical Package for the Social Sciences) 16.0 software (Chicago, IL, USA). For comparisons of two groups, differences were tested using independent Student's *t*-test. For more than two groups, data were compared by one-way analysis of variance (ANOVA), followed by post hoc analysis using the LSD (least significant difference) test. $P < 0.05$ was considered significant.

Results

Selective Blockade of Kv1.3 by Psora-4 and MgTX Promoted NPC Neuronal Differentiation

To test the morphological development of cells during NPC differentiation, we first identified NPCs, neurons, and astrocytes by immunostaining. Cells were immunolabeled with the NPC marker nestin, the neuronal markers β-III-tubulin and MAP2, and the astroglial marker GFAP (Figure 1A).

Next, we studied the effect of Psora-4 on NPC differentiation by exposing cultured NPCs to differentiation medium with Psora-4 in a range of concentrations: 0, 5, 10, 20, and 50 nM. After 5 days of differentiation, cells were labeled by immunostaining with anti-β-III-tubulin and anti-GFAP antibodies (Figure 1B). The total numbers of cells and of immunolabeled cells were counted in each well, and the cell ratios are expressed as the percentage of total cells. Various concentrations of Psora-4 influenced the percentages of β-III-tubulin-positive neurons and GFAP-positive astrocytes. Psora-4 at 10 nM significantly increased the proportion of neurons from 31.5 ± 0.7% to 37.1 ± 0.5% ($n = 3$, $P < 0.01$) and caused an obvious decrease in the percentage of astrocytes from 60.4% ± 3.0% to 52.9 ± 2.5% ($n = 3$, $P < 0.05$, Figure 1C). Treatment with 50 nM Psora-4 caused the percentage of neurons to decrease

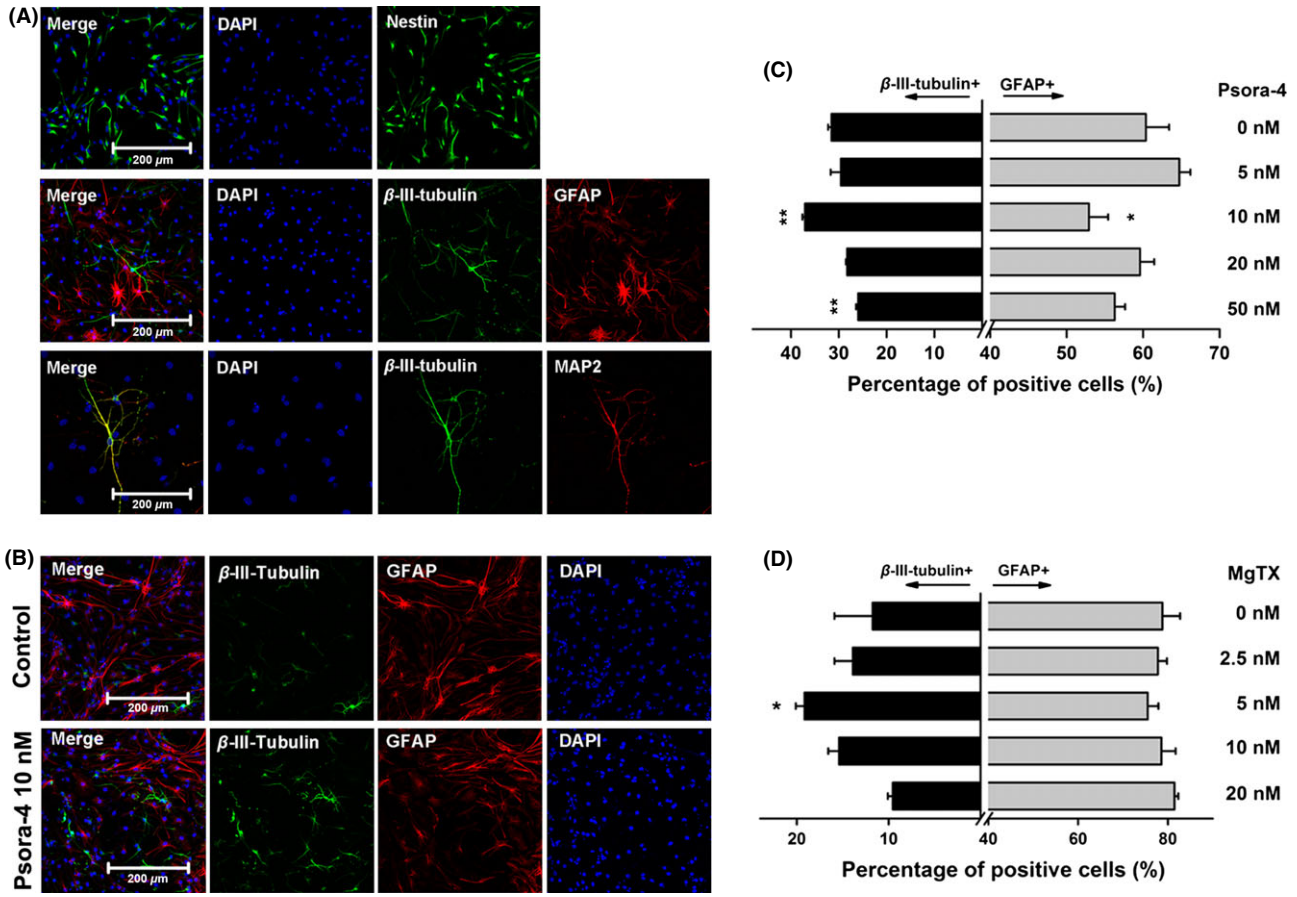

Figure 1 Psora-4 or MgTX promoted the differentiation of neural progenitor cells (NPCs) toward a neuronal lineage. (**A**) Identification of NPCs and differentiated cells derived from NPCs by immunocytochemistry. The NPCs were labeled with antibody for nestin (green) at Day 0, and the differentiated cells were labeled with antibodies for β-III-tubulin (green), MAP2 (red) and GFAP (red) at Day 5. Nuclei were stained with DAPI (blue). (**B**) Example images of cells immunostained at Day 5 with or without Psora-4 (10 nM). (**C**) and (**D**) Various concentrations of Psora-4 or MgTX affect NPC neuronal differentiation. The percentage of positive cells was calculated in relation to the total number of cells, visualized by DAPI staining of the nuclei. $^{**}P < 0.01$, $^{*}P < 0.05$.

to 25.9% ± 0.5% (n = 3, $P < 0.01$). These results suggest that 10 nM Psora-4 could promote NPC differentiation into neurons.

Another high-affinity polypeptide blocker of Kv1.3, MgTX, was also applied to test its effect on NPC differentiation. MgTX was added to NPC differentiation medium in a range of concentrations: 0, 2.5, 5, 10, and 20 nM. The percentage of β-III-tubulin-positive cells was counted at Day 5. We found that MgTX at 5 nM significantly increased the percentage of β-III-tubulin-positive neurons, from 11.8 ± 4.2% to 19.2 ± 0.9% (n = 3, $P < 0.05$), but there was no significant effect on the number of GFAP-positive astrocytes (Figure 1D). These results indicate that the effect of MgTX on regulating NPC neuronal differentiation was similar to that of Psora-4.

Selective Silencing of Kv1.3 Through shRNA in NPCs Resulted in Increased Neuronal Differentiation Efficiency

To further establish that the mechanism by which Psora-4 affects NPC differentiation is through Kv1.3, not direct action of the compound itself, Kv1.3-silenced NPC lines were made through shRNA interference as a parallel experiment (Figure 2A). Four shRNA sequences were tested (Table 1). Real-time quantitative PCR was used to select a Kv1.3-silenced cell line. The Kv1.3 mRNA expression level in the presence of shRNA-1 was remarkably down-regulated by 85.2 ± 1.7% (n = 4, $P < 0.001$, Figure 2B) compared to the Nonsense shRNA control cell line.

Then, three cell lines, the Kv1.3-silenced NPCs, Blank vector control, and Nonsense control, were subjected to differentiation conditions. Immunofluorescence staining was performed to test the efficiency of neuronal differentiation at Day 5. The Kv1.3-silenced NPCs generated a higher efficiency of neuronal differentiation (26.5 ± 1.4%, percentage of β-III-tubulin-positive cells) than the Nonsense control group (21.6 ± 0.2%, n = 3, $P < 0.05$) or the Blank vector group (20.3 ± 0.8%, n = 4, $P < 0.01$). Furthermore, as with normal NPCs, 10 nM Psora-4 increased the proportion of β-III-tubulin-positive cells in the Nonsense control group to 28.2 ± 1.5% (n = 4, $P < 0.05$) and that in the Blank vector group to 25.0 ± 1.6% (n = 4, $P < 0.05$). Psora-4 showed no significant influence on Kv1.3 silenced NPCs (n = 4, 25.9 ± 0.9%, Figure 2C). We also calculated the percentage of astrocytes, but we found no significant difference (Figure 2D).

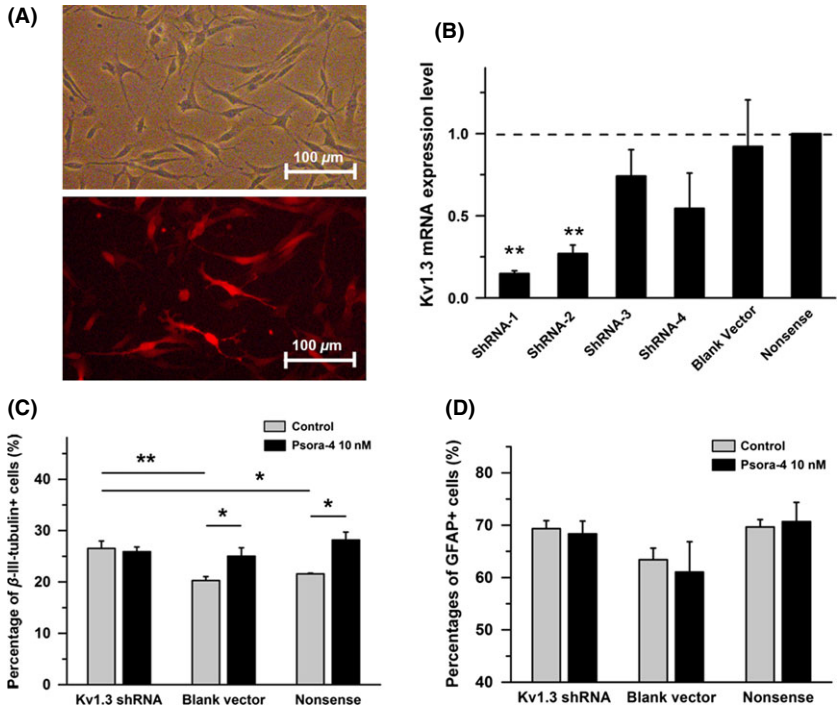

Figure 2 Silencing of Kv1.3 in neural progenitor cells (NPCs) by shRNA interference induced increased differentiation efficiency, consistent with Psora-4 treatment. (**A**) Example images of NPCs infected with shRNA lentiviruses with red fluorescence after flow cytometric sorting. The top panel shows the light field, and the bottom panel shows the red fluorescence in the same field. The cells were plated on Matrigel-coated slides. (**B**) Kv1.3 mRNA expression levels in NPCs with shRNA lentivirus. Relative Kv1.3 mRNA expression was quantified and normalized to the Nonsense control group (n = 4). Nonsense control: NPCs infected with lentivirus containing the nonsense shRNA-sequence. Blank vector: NPCs infected with empty lentivirus vector. (**C**) and (**D**) Differentiation efficiency of NPC cell lines with Kv1.3-shRNA toward neuron lineage or astrocyte lineage. The data were calculated at Day 5 in differentiation condition (n = 4). $^{**}P < 0.01$, $^{*}P < 0.05$.

These results suggest that the Kv1.3 channel participated in the fate decision during NPC differentiation.

Neurons Differentiated with Kv1.3 Blockade Developed Greater Morphological Maturity

As time passes, newborn neurons derived from NPCs show more mature morphology. The neurites become more extensive, and the branch number of each neuron increases. Neuronal morphology at days 5, 10, and 14 are shown in Figure 3A. To quantify the degree of neuronal maturity, the branch number and neurite length were calculated. The differentiated cells were immunostained at Day 5. Both the total branch number and the length of the longest neurite were measured for β-III-tubulin-positive cells. With Psora-4 treatment (10 nM), the percentage of multiple-neurite neurons (more than two branches) was significantly increased, from 66.5 ± 10.0% to 75.9 ± 10.8% (n = 3, $P < 0.01$, Figure 3B left). The average length of the longest neurite did not change between the control group (53.5 ± 5.3 μm) and the Psora-4 group (n = 4, 57.2 ± 3.5 μm, Figure 3B right). These results indicate that Psora-4 could help newborn neurons to form a more complicated neurite structure.

During neurogenesis, not all of the newborn cells can be incorporated into the nervous system. Most of the NPC offspring (especially neurons) fail to mature and instead undergo apoptosis [24,25]. Cheyne et al. [26] found that the newborn neurons with large somata and long dendrites tended to integrate into the neuronal network. We observed cells at days 5, 10, and 14 using immunostaining for β-III-tubulin and GFAP antibodies. Some immature-like neurons had short and sparse dendrites (Figure 3C, white arrows), while some mature-like neurons had long and extensive dendrites (orange arrows). Those mature-like neurons were then manually counted. The percentage of mature-like neurons was significantly increased by treatment with 10 nM Psora-4 (n = 5, $P < 0.01$ at Day 5, $P < 0.05$ at days 10 and 14, Figure 3D). Similarly, MgTX (5 nM) significantly increased the percentage of mature-like neurons from 0.17 ± 0.03% to 0.24 ± 0.01% (n = 3, $P < 0.05$, Figure 3E). These results indicate that selective blockade of Kv1.3 could promote the maturation and integration of newborn neurons during NPC differentiation.

Psora-4 Promoted the Preliminary Functional Maturation of NPC-Derived Neurons

To determine whether newborn neurons derived from NPCs could develop the essential functions of neurons, we performed whole-cell patch clamping (Figure 4B) and recorded the electrophysiological activities of neurons in the absence (Figure 4A, left) and the presence Psora-4 (10 nM) group (Figure 4A, right). Neurons were identified first by their morphology and then by their ability

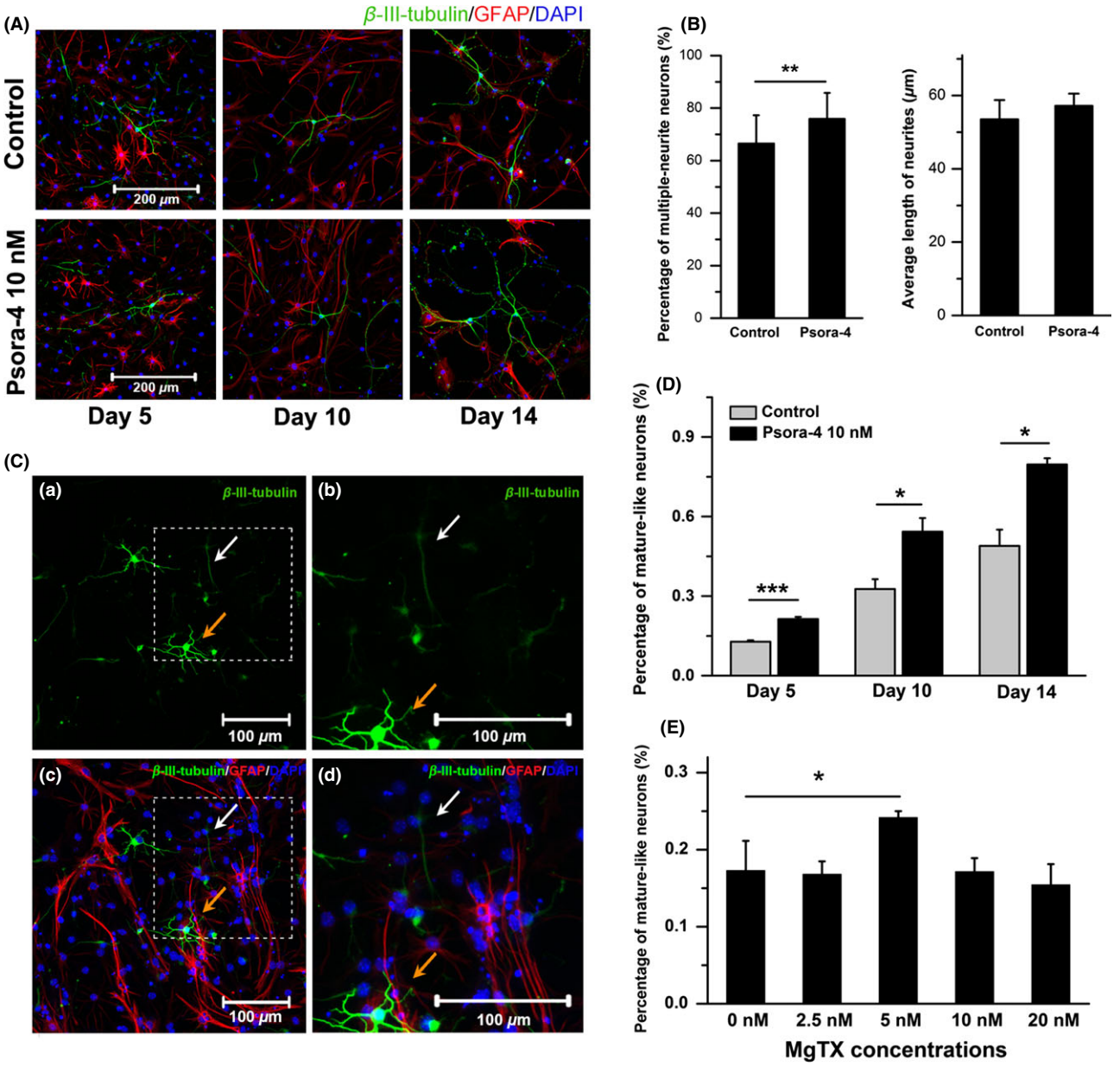

Figure 3 Newborn neurons derived from neural progenitor cells (NPCs) in the presence of Psora-4 (10 nM) developed more mature morphology. (**A**) Immunocytochemistry images of NPC offspring with or without Psora-4 at days 5, 10, and 14. (**B**) Psora-4 influenced the morphology of newborn neurons. Left, percentage of neurons with multiple neurites (n = 3). Right, average neurite length (n = 4). At least 150 neurons were measured using ImageJ in each independent experiment. (**C**) Mature-like and immature-like neurons at Day 5 of NPC neuronal differentiation. (**a**) Low-power image of mature-like neurons with long and extensive dendrites (orange arrow) and immature-like neurons with thin and sparse dendrites (white arrow). (**b**) High-power image of boxed region in panel **a**. (**c**) Low-power image of neurons (green) and astrocytes (red). This shows the same field as the image in panel **a**. (**d**) High-power image of the boxed region in panel **c**. (**D**) Psora-4 increased the percentage of mature neuron candidates at days 5, 10, and 14 in differentiation condition. (n = 5). (**E**) MgTX (5 nM) increased the percentage of mature-like neurons at Day 5 (n = 3). ***$P < 0.001$, **$P < 0.01$, *$P < 0.05$.

to spike in response to depolarizing steps of current injection. In current-clamp recordings, injection of step currents (−20 pA to 50 pA) induced multiple action potentials (APs) (Figure 4A b, f). We also recorded continuous spontaneous APs from neurons in both groups (Figure 4A a, e). Depolarizing voltage steps in voltage-clamp mode elicited mature outward K^+ currents and inward Na^+ currents (Figure 4A e, d, g, h). These results indicate that neurons differentiated either with or without Psora-4 could develop mature electrophysiological functions.

To detect the mature time course of the electrophysiological function of neurons, we manually selected three main periods based on the progress toward neuronal maturity: days 5–10, days 13–16, and days 20–24. Representative experiments are shown in Figure 5A. As time passed, neurons generated increasing outward

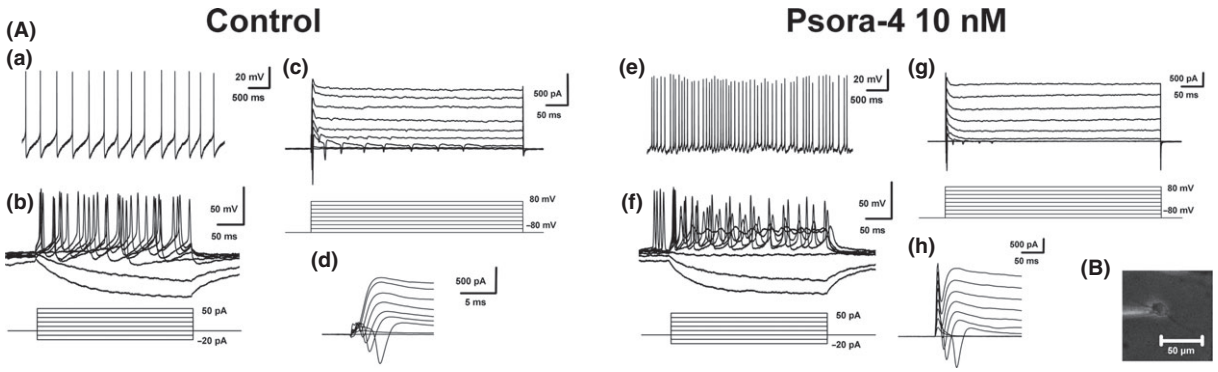

Figure 4 Neuron-like cells differentiated with or without Psora-4 (10 nM) displayed mature electrophysiological characteristics. (**A**) Representative electrophysiological recordings of neurons from control and Psora-4 group, respectively. Spontaneous and induced continuous action potentials (APs) were recorded under current clamp (shown in **a**, **b**, **e**, and **f**). Mature positive K^+ and negative Na^+ currents were recorded under voltage-clamp (shown in **c**, **d**, **g**, and **h**). (**B**) A microscopic image showing whole-cell patch-clamp recording of a neuron at Day 14.

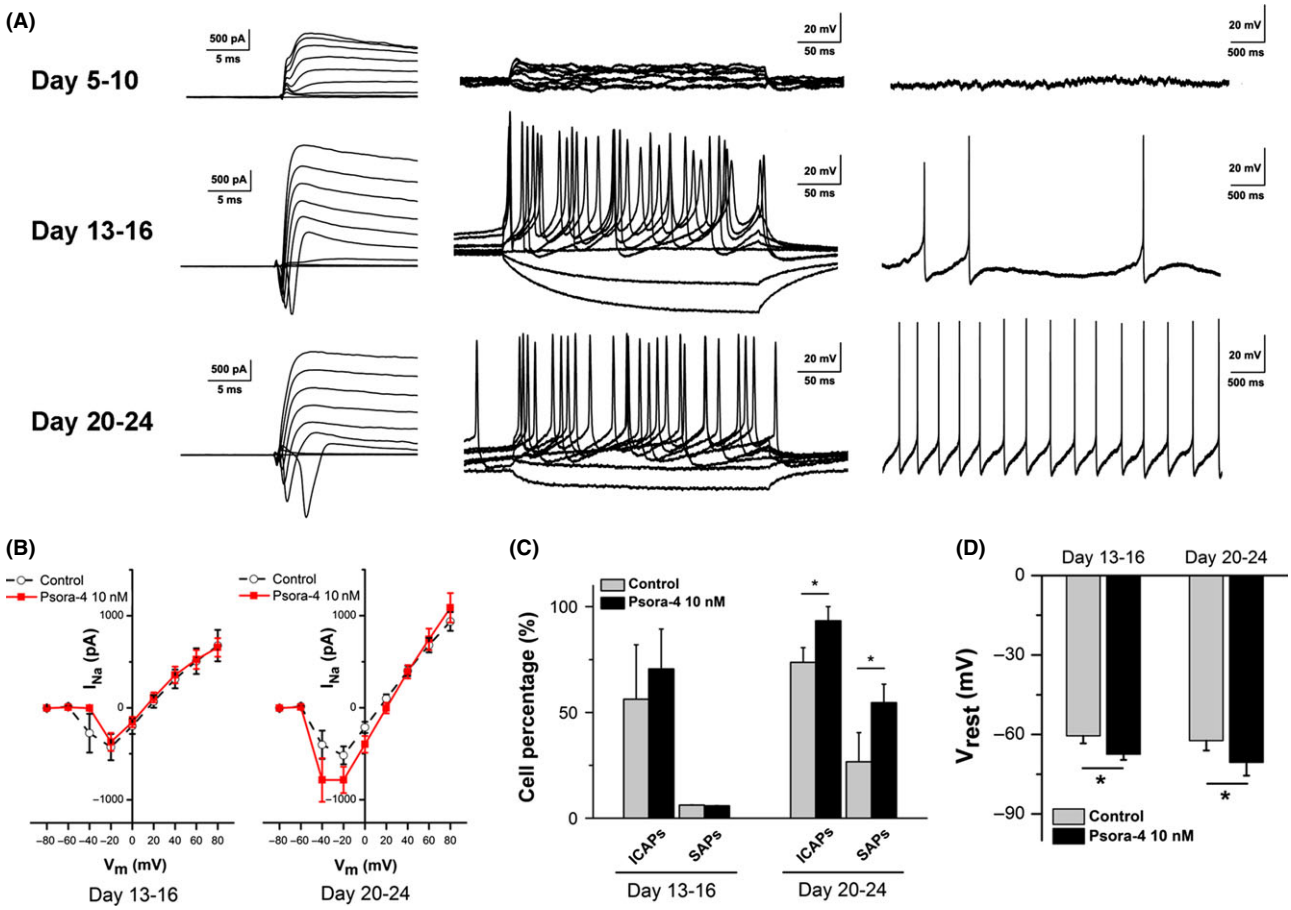

Figure 5 Newborn neurons derived from neural progenitor cells (NPCs) in the Psora-4 (10 nM) group developed more mature electrophysiological properties. (**A**) Typical electrophysiological recordings from the three main differentiation periods (days 5–10, 13–16 and 20–24). The left panel shows K^+ and Na^+ currents, the middle panel shows induced action potentials (APs), and the right panel shows spontaneous APs. (**B**) Current-voltage relationships for Na^+ current (I_{Na}) at days 13–16 (left) and days 20–24 (right). The I_{Na} value at days 20–24 was significantly increased in the presence of Psora-4 (n = 19). I_{Na} was measured as the peak inward current. (**C**) Psora-4 increased the percentage of neurons that fired induced continuous APs (ICAPs) and spontaneous APs (SAPs) at days 20–24. (**D**) Neurons differentiated with Psora-4 developed more hyperpolarized rest membrane potentials (V_{rest}) both at days 13–16 (control n = 18, Psora-4 n = 17) and at days 20–24 (control n = 19, Psora-4 n = 18). *$P < 0.05$.

K^+ and inward Na^+ currents (Figure 5A, left). In agreement with these results, induced and spontaneous APs increased in frequency and gradually became more continuous (Figure 5A, middle, right).

The electrophysiological properties of NPC-derived neurons were quantified and compared between the control and Psora-4 (10 nM) groups. The influence of Psora-4 on neuronal function increased obviously over time. In the early periods, little difference was recorded at days 5–10 (data not shown) and days 13–16 (shown as the Na^+ I–V curves, Figure 5B, left). In the late period, days 20–24, the peak amplitude of Na^+ currents (at −20 mV) of Psora-4 neurons (−518 ± 97 pA, n = 19) was significantly larger than those of control neurons (−398 ± 92 pA, n = 17, $P < 0.05$, Figure 5B, right). However, there was little difference at the peak amplitude of K^+ currents between the two groups (Table 2). These results indicate that Psora-4 helps newborn neurons to develop larger sodium currents, which mainly participated in the firing of action potentials.

Consistent with the voltage-clamp recordings, current-clamp data showed that neurons differentiated with Psora-4 (10 nM) were more mature than control neurons. During the late period, days 20–24, the percentage of neurons that fired induced continuous APs (ICAPs) was significantly increased in the presence of Psora-4, from 73.7 ± 7.0% (14 of 17 neurons) to 93.3 ± 6.7% (18 of 19 neurons, $P < 0.05$, Figure 5C). Psora-4 also significantly increased the percentage of neurons that fired spontaneous APs (SAPs), from 26.7 ± 13.8% (five of 17 neurons) to 54.7 ± 8.7% (10 of 19 neurons, $P < 0.05$, Figure 5C). Additional characteristics such as AP peak value, AP frequency, and after-hyperpolarization (AHP) amplitude were also calculated, and no significant difference was found (Table 2). These results suggest that neurons in the presence of Psora-4 could develop more mature properties and become functional earlier than control neurons.

Neurons differentiated in the presence of Psora-4 (10 nM) exhibited more hyperpolarized resting membrane potentials (V_{rest}), which is determined by the relative ionic concentrations and permeabilities. During the early period, days 13–16, the average V_{rest} of neurons in the Psora-4 group was −67.4 ± 2.1 mV (n = 17), which is significantly more hyperpolarized than the V_{rest} of the control group, −60.5 ± 2.8 mV (n = 18, $P < 0.05$, Figure 5D). Neurons in the late period, days 20–24, also showed significant differences, with a V_{rest} of −62.3 ± 3.7 mV in the control group (n = 19) and a V_{rest} of −70.5 ± 5.0 mV in the Psora-4 group (n = 18, $P < 0.05$, Figure 5D). These results suggest that Psora-4 could help newborn neurons to generate a functional ion channel distribution.

Discussion

The above results suggest that Kv1.3 blockers can promote NPC neuronal differentiation and maturation. First, Psora-4, a small-molecule selective blocker for Kv1.3, was found to increase the differentiation efficiency of NPCs in a concentration-dependent manner. Another Kv1.3 blocker, MgTX, was also found to influence NPC neuronal differentiation. Then, shRNA targeting Kv1.3 was used in NPCs as a parallel experiment, generating an increased proportion of neurons, consistent with the Psora-4 and MgTX results. Furthermore, Psora-4 was also found to contribute to the morphological maturation of neurons. Finally, functional analysis indicated that NPC-derived neurons that were differentiated in the presence of Psora-4 developed greater electrophysiological maturity.

Previous studies had shown that neurogenesis could be regulated by different kinds of factors, including extrinsic molecules [27,28], physical stimuli [29], and intracellular regulators [30]. However, the role of ion channels in NPC differentiation is still poorly understood, although both the ion channel species and the membrane potential of NPCs change during differentiation [31]. Our results demonstrate that selective blockade or silencing Kv1.3, a voltage-gated potassium channel, promoted NPC neuronal differentiation and maturation. Tetraethylammonium, a broad-spectrum inhibitor of voltage-gated potassium channels [32], was also tested, but it was cytotoxic to NPCs (data not shown). Previously, Kv1.3 blockade was reported to inhibit the proliferation of oligodendrocyte progenitor cells [14]. Because the offspring of differentiating NPCs are mainly composed of neurons, astrocytes, and oligodendrocytes, Kv1.3 blockade or silencing may act in neurogenesis through the blockade of proliferation or differentiation to oligodendrocytes. The cellular mechanism by which inhibition of Kv1.3 promotes NPC neuronal differentiation requires further study.

Because of their capacity for self-renewal and differentiation, NPCs represent a promising approach for achieving CNS tissue repair in neurodegenerative diseases such as MS, a chronic

Table 2 Electrophysiological properties of neurons recorded at days 13–16 and days 20–24

	Days 13–16		Days 20–24	
	Control	Psora-4 10 nM	Control	Psora-4 10 nM
Neurons (n)	16	17	19	18
I_{Na} (nA)	−0.441 ± 0.172	−0.380 ± 0.123	−0.657 ± 0.206	−0.898 ± 0.216*
I_K (nA)	1.76 ± 0.22	1.71 ± 0.28	1.81 ± 0.18	2.11 ± 0.27
V_{rest} (mV)	−60.5 ± 2.8	−67.4 ± 2.1*	−62.3 ± 3.7	−70.5 ± 5.0*
AP peak (mV)	46.9 ± 8.7	54.9 ± 5.6	57.7 ± 9.3	63.5 ± 7.6
AHP (mV)	−14.7 ± 3.8	−14.3 ± 2.8	−11.0 ± 0.8	−11.6 ± 2.4
Induced AP frequency (Hz)	35.9 ± 3.9	30.4 ± 0.9	27.0 ± 3.6	25.1 ± 1.7

I_{Na} was measured as peak inward current, and I_K was measured as peak outward current. Action potential (AP) peak and after-hyperpolarization (AHP) values were measured in the first action potential of the spike train. Induced AP frequency was measured on those neurons that fired induced continuous APs. *$P < 0.05$.

inflammatory multifocal demyelinating disorder [6]. However, the clinical application of NPC engraftment has been limited by challenges such as poor cell sources and low differentiation efficiency. As a potential treatment for MS, Kv1.3 blockers were reported to ameliorate disease in animal models of MS [11]. In this study, we report that Psora-4, a selective molecular blocker of Kv1.3 channels, promotes neuronal differentiation and maturation of NPCs. Our studies partially explain the underlying mechanism of Kv1.3 blockade-based MS therapy at the cellular level. Increasing the activity of NPCs to an appropriate degree, instead of NPCs transplantation, may represent a novel treatment for CNS disorders. In this study, fetal mice NPCs were used for reasons of cell feasibility and quantity. To address the age factor in demyelinating diseases, our next research step would focus on applying Psora-4 to adult NPCs *in vivo* and *in vitro*.

Psora-4 is a derivative of 5-methoxypsoralen that binds to a water-filled cavity below the selectivity filter of Kv1.3 [33]. Psora-4 can be synthesized simply, and it causes little acute toxicity to cells [22]. Our results show that 10 nM Psora-4 increased the NPC neuronal differentiation efficiency and promoted newborn neurons to develop mature functions. Neurons derived from NPCs in the presence of Psora-4 had normal electrophysiological activities (Figure 4). The AP properties (including AP peak value, AHP, and AP frequency) of neurons in the Psora-4 group were not obviously different from those of the control group (Table 2). Thus, Psora-4 has a bright prospect for further understanding NPC activity and for clinical therapies for MS. Liebau et al. [34] reported those Kv1 ion channel subfamily, included Kv1.1, Kv1.2, Kv1.3, and Kv1.4, expressed in NPCs. In our present study, Psora-4 at a higher concentration (50 nM) produced a more negative effect. This may be because the higher concentration of Psora-4 blocked other Kv1 channels such as Kv1.2, thus causing changes in membrane osmotic pressure and cytotoxicity [22].

During development and also in the adult brain, only a subset of newborn neurons derived from NSCs integrate into the circuitry, and most of these neurons undergo death at immature stages [25]. Until now, however, the survival and maturation of newborn neurons were hard to evaluate through biochemical methods because of the lack of a convincing cell marker. In this study, we detected the maturation of newborn neurons through the quantification of morphology and electrophysiology. Our results indicated that NSCs in the presence of Psora-4 (10 nM) generated more mature neurons, showing increased maturity both morphologically and electrophysiologically. Previous studies reported that Kv1.3 blockade promoted neurotransmitter release and caused cell membrane depolarization [35]. The cell membrane depolarization would lead to the activation of voltage-gated Ca^{2+} channels which had been reported to play a functional role during the early neuron development [36]. Thus, Kv1.3 inhibitors may promote the maturation of newborn neurons by increasing intracellular Ca^{2+} concentration. However, because low functional Ca^{2+} currents were recorded in nestin-positive NPCs, the voltage-gated Ca^{2+} channel should not participate in neuronal fate determination [37,38].

In conclusion, we first uncovered that selective blockade of Kv1.3 ion channel could promote NPC neuronal differentiation and maturation. Our results partially explain the therapeutic mechanisms by which Kv1.3 blockers have been used to treat neurological diseases such as MS. Furthermore, the small-molecule selective Kv1.3 blocker Psora-4 has the potential to be developed into a clinical treatment for MS. However, more intensive studies are still needed. Applying Psora-4 to MS animal models *in vivo* will be the next step in our research.

Acknowledgments

This work was supported by the National Basic Research Program of China, 973 Program (2012CB966404), the National Natural Science Foundation of China (81171037), and the Science and Technology Programme of Guangzhou Municipal Government (2014J4100221).

Conflict of Interest

The authors declare no conflict of interest.

References

1. Song HJ, Stevens CF, Gage FH. Neural stem cells from adult hippocampus develop essential properties of functional CNS neurons. *Nat Neurosci* 2002;**5**:438–445.
2. Trapp BD, Peterson J, Ransohoff RM, Rudick R, Mork S, Bo L. Axonal transection in the lesions of multiple sclerosis. *N Engl J Med* 1998;**338**:278–285.
3. Compston A, Coles A. Multiple sclerosis. *Lancet* 2008;**372**:1502–1517.
4. Noseworthy JH, Lucchinetti C, Rodriguez M, Weinshenker BG. Multiple sclerosis. *N Engl J Med* 2000;**343**:938–952.
5. Coles AJ, Twyman CL, Arnold DL, et al. Alemtuzumab for patients with relapsing multiple sclerosis after disease-modifying therapy: A randomised controlled phase 3 trial. *Lancet* 2012;**380**:1829–1839.
6. Martino G, Pluchino S. The therapeutic potential of neural stem cells. *Nat Rev Neurosci* 2006;**7**:395–406.
7. Akiyama Y, Honmou O, Kato T, Uede T, Hashi K, Kocsis JD. Transplantation of clonal neural precursor cells derived from adult human brain establishes functional peripheral myelin in the rat spinal cord. *Exp Neurol* 2001;**167**:27–39.
8. Hofstetter CP, Holmstrom NA, Lilja JA, et al. Allodynia limits the usefulness of intraspinal neural stem cell grafts; directed differentiation improves outcome. *Nat Neurosci* 2005;**8**:346–353.
9. Uccelli A, Laroni A, Freedman MS. Mesenchymal stem cells for the treatment of multiple sclerosis and other neurological diseases. *Lancet Neurol* 2011;**10**:649–656.
10. Karussis D, Karageorgiou C, Vaknin-Dembinsky A, et al. Safety and immunological effects of mesenchymal stem cell transplantation in patients with multiple sclerosis and amyotrophic lateral sclerosis. *Arch Neurol* 2010;**67**:1187–1194.
11. Rangaraju S, Chi V, Pennington MW, Chandy KG. Kv1.3 potassium channels as a therapeutic target in multiple sclerosis. *Expert Opin Ther Targets* 2009;**13**:909–924.
12. Storey NM, Gomez-Angelats M, Bortner CD, Armstrong DL, Cidlowski JA. Stimulation of Kv1.3 potassium channels by death receptors during apoptosis in Jurkat T lymphocytes. *J Biol Chem* 2003;**278**:33319–33326.
13. Szabo I, Zoratti M, Gulbins E. Contribution of voltage-gated potassium channels to the regulation of apoptosis. *FEBS Lett* 2010;**584**:2049–2056.
14. Chittajallu R, Chen Y, Wang H, et al. Regulation of Kv1 subunit expression in oligodendrocyte progenitor cells and their role in G1/S phase progression of the cell cycle. *Proc Natl Acad Sci USA* 2002;**99**:2350–2355.
15. Colley B, Tucker K, Fadool DA. Comparison of modulation of Kv1.3 channel by two receptor tyrosine kinases in olfactory bulb neurons of rodents. *Receptors Channels* 2004;**10**:25–36.
16. Arcangeli A, Crociani O, Lastraioli E, Masi A, Pillozzi S, Becchetti A. Targeting ion channels in cancer: A novel frontier in antineoplastic therapy. *Curr Med Chem* 2009;**16**:66–93.
17. Schmitz A, Sankaranarayanan A, Azam P, et al. Design of PAP-1, a selective small molecule Kv1.3 blocker, for the suppression of effector memory T cells in autoimmune diseases. *Mol Pharmacol* 2005;**68**:1254–1270.
18. Wang T, Lee MH, Johnson T, et al. Activated T-cells inhibit neurogenesis by releasing granzyme B: Rescue by Kv1.3 blockers. *J Neurosci* 2010;**30**:5020–5027.
19. Wang T, Lee MH, Choi E, et al. Granzyme B-induced neurotoxicity is mediated via activation of PAR-1 receptor and Kv1.3 channel. *PLoS One* 2012;**7**:e43950.
20. Duque A, Gazula VR, Kaczmarek LK. Expression of Kv1.3 potassium channels regulates density of cortical interneurons. *Dev Neurobiol* 2013;**73**:841–855.

21. Franklin RJ, Ffrench-Constant C. Remyelination in the CNS: From biology to therapy. *Nat Rev Neurosci* 2008;**9**:839–855.
22. Vennekamp J, Wulff H, Beeton C, et al. Kv1.3-blocking 5-phenylalkoxypsoralens: A new class of immunomodulators. *Mol Pharmacol* 2004;**65**: 1364–1374.
23. Wang L, Wang L, Huang W, et al. Generation of integration-free neural progenitor cells from cells in human urine. *Nat Methods* 2013;**10**:84–89.
24. Dayer AG, Ford AA, Cleaver KM, Yassaee M, Cameron HA. Short-term and long-term survival of new neurons in the rat dentate gyrus. *J Comp Neurol* 2003;**460**: 563–572.
25. Sierra A, Encinas JM, Deudero JJ, et al. Microglia shape adult hippocampal neurogenesis through apoptosis-coupled phagocytosis. *Cell Stem Cell* 2010;**7**:483–495.
26. Cheyne JE, Grant L, Butler-Munro C, Foote JW, Connor B, Montgomery JM. Synaptic integration of newly generated neurons in rat dissociated hippocampal cultures. *Mol Cell Neurosci* 2011;**47**:203–214.
27. Ng SY, Bogu GK, Soh BS, Stanton LW. The Long noncoding RNA RMST interacts with SOX2 to regulate neurogenesis. *Mol Cell* 2013;**51**:349–359.
28. Ge S, Pradhan DA, Ming GL, Song H. GABA sets the tempo for activity-dependent adult neurogenesis. *Trends Neurosci* 2007;**30**:1–8.
29. Toni N, Teng EM, Bushong EA, et al. Synapse formation on neurons born in the adult hippocampus. *Nat Neurosci* 2007;**10**:727–734.
30. Gao FB. Posttranscriptional control of neuronal development by microRNA networks. *Trends Neurosci* 2008;**31**:20–26.
31. Yasuda T, Adams DJ. Physiological roles of ion channels in adult neural stem cells and their progeny. *J Neurochem* 2010;**114**:946–959.
32. Armstrong CM. Interaction of tetraethylammonium ion derivatives with the potassium channels of giant axons. *J Gen Physiol* 1971;**58**:413–437.
33. Leanza L, Henry B, Sassi N, et al. Inhibitors of mitochondrial Kv1.3 channels induce Bax/Bak-independent death of cancer cells. *EMBO Mol Med* 2012;**4**:577–593.
34. Liebau S, Propper C, Bockers T, et al. Selective blockage of Kv1.3 and Kv3.1 channels increases neural progenitor cell proliferation. *J Neurochem* 2006;**99**:426–437.
35. Shoudai K, Nonaka K, Maeda M, et al. Effects of various K+ channel blockers on spontaneous glycine release at rat spinal neurons. *Brain Res* 2007;**1157**:11–22.
36. Spitzer NC. Electrical activity in early neuronal development. *Nature* 2006;**444**:707–712.
37. Cai J, Cheng A, Luo Y, et al. Membrane properties of rat embryonic multipotent neural stem cells. *J Neurochem* 2004;**88**:212–226.
38. D'Ascenzo M, Piacentini R, Casalbore P, et al. Role of L-type Ca2+ channels in neural stem/progenitor cell differentiation. *Eur J Neurosci* 2006;**23**:935–944.

